Gravity and flexure models of the San Luis, Albuquerque, and Tularosa basins in the Rio Grande rift, New Mexico, and southern Colorado

Chloe Peterson and Mousumi Roy
2005, pp. 105-114. https://doi.org/10.56577/FFC-56.105

in:

Geology of the Chama Basin, Lucas, Spencer G.; Zeigler, Kate E.; Lueth, Virgil W.; Owen, Donald E.; [eds.], New Mexico Geological Society 56th Annual Fall Field Conference Guidebook, 456 p. https://doi.org/10.56577/FFC-56

This page is intentionally left blank to maintain order of facing pages.

GRAVITY AND FLEXURE MODELS OF THE SAN LUIS, ALBUQUERQUE, AND TULAROSA BASINS IN THE RIO GRANDE RIFT, NEW MEXICO, AND SOUTHERN COLORADO

CHLOE PETERSON AND MOUSUMI ROY
Department of Earth and Planetary Sciences, University of New Mexico, Albuquerque, NM 87131

Abstract.—The Rio Grande rift is a Cenozoic continental rift zone that trends south from central Colorado through New Mexico and merges with a broader extensional zone in west Texas and Chihuahua, Mexico. The net upper crustal extension increases southward along the rift, accompanied by a southward-widening of the rift from a narrow zone encompassing a single basin in the north to a wide zone of multiple, laterally adjacent basins to the south. In this study we model the isostatic responses of the lithosphere to extension along the Rio Grande rift, and compare and contrast this response in the San Luis and Albuquerque basins in the narrow part of rift and the Tularosa basin in the wider region of the rift. Our flexural isostatic models are based on a joint-inversion of gravity and deflection data along the footwalls of major basin-bounding faults. The main difficulty in constraining isostatic response to extension in the Rio Grande rift is a lack of constraints on footwall deflection. Our approach is to use topography as a proxy for flexural deflection, and then to compare the estimated end-loads required for plate flexure in the footwall with the end-loads estimated from hanging wall and basin geometry. Using this approach we determine the extent to which flexural isostasy could have generated elevated rift-flanks, and how this process might change along strike. Our results indicate that flexural responses to extension are consistent with rock and surface uplift in the footwalls of the Albuquerque and the Tularosa basins in the central and southern Rio Grande rift. In the San Luis basin, however, although a flexural curve may adequately fit footwall topography, the plate-end loads required for flexure are inconsistent with those inferred from the hanging wall and basin geometries. Additionally, flexure-based estimates of crustal extension agree with geologic estimates in the Albuquerque and Tularosa basins, but not in the San Luis basin. We infer therefore, that rift-flank uplift due to flexure is likely only in the central and southern parts of the Rio Grande rift; to the north, we infer an additional (perhaps pre-rift) contribution to rift-flank topography.

INTRODUCTION

Cenozoic tectonism along the eastern margin of the Colorado Plateau is characterized by a period of crustal shortening and surface uplift in the Laramide orogeny (70-40 Ma), followed by a middle-Tertiary period of voluminous caldera-complex magmatism ("ignimbrite flare-up") and Neogene (35-20 Ma) onset of crustal extension in the Rio Grande rift. These tectonic events have all variably contributed to the present-day physiography of the Rio Grande rift and surrounding regions (e.g., Laramide high topography in the Southern Rocky Mountains, Gregory and Chase, 1994; epeirogenic rock-uplift driven by middle-Tertiary magmatic modification of the lithosphere, Roy et al., 2004; and flexural uplift of rift-flanks due to extension, Roy et al., 1999; Brown and Phillips, 1999; House et al., 2003). In this paper we focus on and explore flexural responses to extension in the Rio Grande rift and determine to what extent flexure is a valid process for generating elevated rift-flanks and evaluate how this process may have varied along-strike. The main difficulty in constraining isostatic response to extension in the Rio Grande rift is a lack of constraints on footwall deflection. Our approach is to use topography as a proxy for flexural deflection (e.g. Roy et al., 1999), and then to compare the estimated end-loads required for plate flexure with end-loads estimated from hanging wall and basin geometry. Additionally, we compare flexure-based estimates of crustal extension with geologic estimates to determine the plausibility of the flexure model. Using this approach, we determine the extent to which flexural isostasy could have generated elevated rift-flanks, and how this process may have varied along strike in the Rio Grande rift.

Extension in the Rio Grande rift has created a corridor of thin crust (30-35 km) at the eastern margin of the Colorado Plateau, which is surrounded by regions of thicker (40-45 km) crust (Keller et al., 1990). The Rio Grande Rift region is underlain by a zone of anomalously slow upper mantle seismic velocities (Dueker et al., 2001; Humphreys et al., 2003; West et al., 2004), but the mantle expression of the extensional processes that formed the rift remains enigmatic and is the subject of a great deal of debate. The generally high heatflow and very young magmatism of the Rio Grande rift region (Sanford et al., 1995; Balch et al., 1997) are consistent with elevated upper mantle temperatures and the presence of partial melt in the lithosphere beneath the rift. Recent seismic images across the Rio Grande rift suggest that the anomalously slow upper mantle velocities beneath the rift may be due to small-scale convection in the asthenospheric upper mantle (Gao et al, 2004; West et al, 2004), which would imply thin (hence relatively weak) lithosphere beneath the rift (Wilson et al., 2005). Although our study cannot constrain upper mantle physical properties, determining the effective rigidity of the lithosphere in response to upper crustal extension will examine strength properties of the plate. Additionally, along-strike variations in effective rigidity may provide clues on how crustal extension is related to upper mantle processes in the region.

We model the isostatic responses to extension using a joint inversion of gravity and deflection data for best-fitting flexural deflection of the footwall blocks of major rift-bounding normal faults of three basins in the Rio Grande rift—the San Luis basin, the Albuquerque basin, and the Tularosa basin (Fig. 1). In our study we assume that elevated rift-flank topography may be used as a proxy for deflection, but we only accept the flexural response

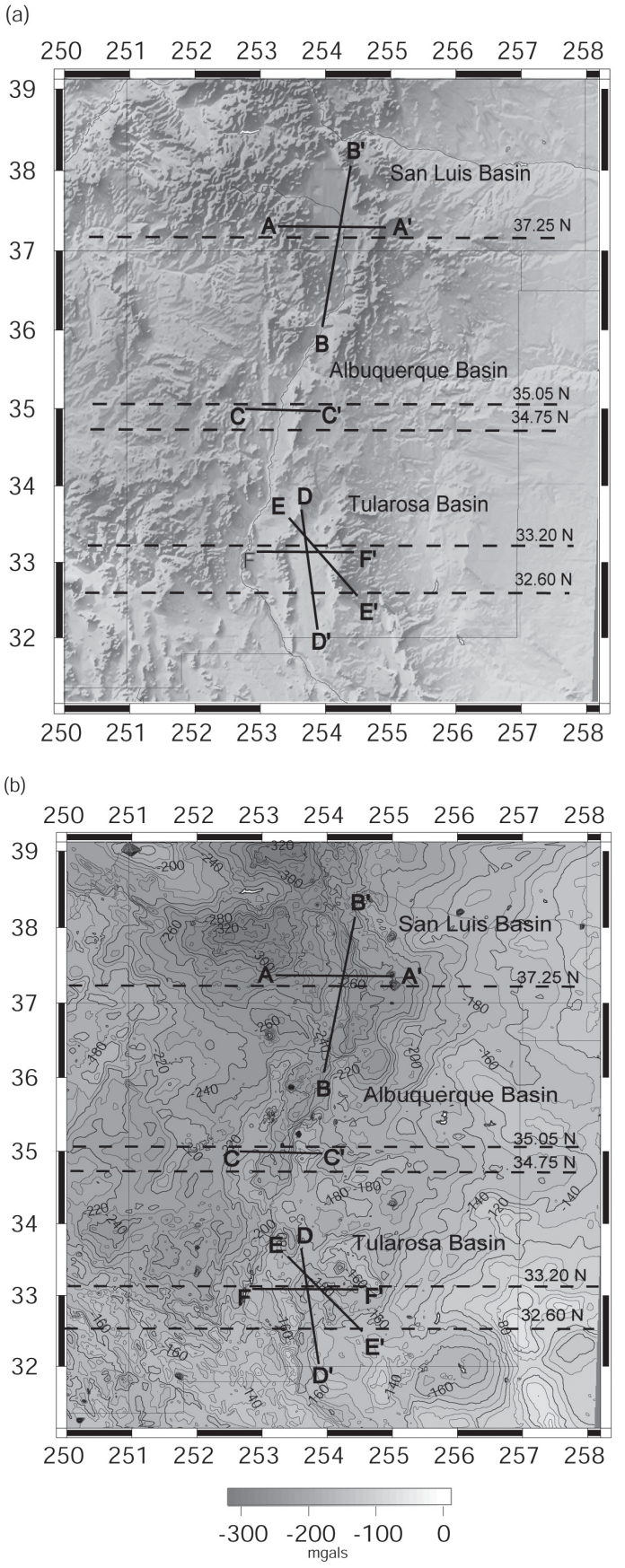

thus calculated as a valid model if the plate end-loads required for flexure are comparable with those estimated from basin geometry and geologic observations on extension. This allows us to quantitatively consider flexure as a process even without the availability of constraints on rift-flank tilting/deflection. (The Española basin, which is between the San Luis and Albuquerque basins, is ignored here because footwall topography in this basin is complicated by the presence of the Jemez volcanic edifice.) To quantify the amount and distribution of loads on the plate due to rifting and basin formation, we first create gravity models of basin geometries that are compared to previous models and complimentary geophysical and geologic datasets. These are followed by 2D flexural modeling based on a joint-inversion of gravity and defection along profiles across the footwall blocks of the rift basins. We evaluate our findings by considering the match between the plate loads required to flexurally uplift the footwall rift-flank with those estimated from the basin geometries and extension.

We find that flexural responses to extension can explain rock (and surface) uplift in the footwall flanks of the Albuquerque and Tularosa basins, but not in the San Luis basin in the northern Rio Grande rift. Estimates of the amount of upper crustal thinning based on the plate geometries inferred in our flexure models are consistent with geologic estimates for the Albuquerque and Tularosa basins, but not for the San Luis basin. Our results suggest that flexure is a viable process for generating rift-flank footwall topography (rift-flank uplift) in the central and southern parts of the Rio Grande rift where the amounts of crustal extension are significant. In the northern, narrow part of the rift, extension is limited and much of the topographic swell surrounding the rift may be due to processes unrelated to extension, e.g., shortening during the Laramide orogeny prior to rifting.

GEOLOGIC SETTING

In the upper crust, the Rio Grande Rift is a series of interconnected, asymmetric grabens and half grabens that stretch from central Colorado through New Mexico, following the crest of the Southern Rocky Mountains (Chapin and Cather, 1994). Complex northeast-striking transfer zones offset the typically opposite-tilting adjacent grabens (Chapin and Cather, 1994). The mode of extension along the rift changes from north to south—in the north the extension is focused in a narrow region encompassing a single basin, whereas in the south the rift is wider and extension is distributed over multiple adjacent basins and the rift merges into the southern Basin and Range province of southern New Mexico and northern Mexico (Cordell, 1978; Kelley and Chapin, 1995). Our study of the flexural response to extension is designed to exploit the along-strike variation in net extension along the Rio Grande Rift: < 6% extension north of the San Luis basin, 12% in the San

FIGURE 1. (a) Topography map of the Rio Grande rift, highlighting the basins used in this study. The gravity profiles used in this study are shown in solid lines while the approximate location of the flexure profiles are shown in dashed lines, including the previous flexure profile from Roy et al. (1999). (b) Bouguer gravity map with profiles used in this study.

Luis basin, 17% in the northern Albuquerque basin, at least 28% in the southern Albuquerque basin and Belen basin, and up to 50% south of the Albuquerque basin (Chapin and Cather, 1994; Russell and Snelson, 1994). This variation in the mode of extension is an essential fact of the evolution of the Rio Grande rift and its relation to the topographic and kinematic evolution of the Southern Rocky Mountains, Colorado Plateau, High Plains, and southern Basin and Range.

GRAVITY MODELS TO DEFINE BASIN GEOMETRY

Bouguer gravity data were obtained from the Pan American Center for Earth and Environmental Studies (PACES) gravity compilation. The dataset is triangulated onto a one kilometer grid using Generic Mapping Tools (Fig. 1b) (Wessel and Smith, 1991). Although the gravity models focus on the subsurface features associated with basins (short wavelength features over distances less than 200 km), profiles spanning up to 10 times these distances are extracted in order to determine regional gravity trends not associated with upper crustal subsurface features. We use topographic data at one kilometer spacing at points co-located with the observed gravity. We extracted a total of six profiles of gravity and topography for our models (Fig. 1). Three east-west profiles spanning from 102° W to 115° W are extracted from the triangulated dataset at ~37.3° N (Profile A, San Luis basin), ~35.0° N (Profile C, Albuquerque basin), and ~33.0° N (Profile F, Tularosa basin). Because the San Luis and the Tularosa basins are significantly less well-studied compared to the Albuquerque basin, three additional profiles are extracted about orthogonal to the east-west profiles that span these basins. Profile B, across the San Luis basin, intersects Profile A at about 37.3° N, 105.5° W and runs approximately north-south (5° east of north, in order to cross several prominent features on the surface of the basin) from 39° N to 31° N (Fig. 1). Profiles D and E, across the Tularosa basin, intersect Profile F at about 33° N, 106.25° W and 33° N, 105.75° W, respectively, and are extracted 10° west of north and 20° west of north, respectively, from 39° N to 31° N (Fig. 1).

Low-order, first to second degree polynomials are fitted to the long-wavelength features in the extracted profiles and detrended from the gravity. These long-wavelength features are likely representative of regional gravity trends caused by sub-basin, Moho and sub-crustal anomalies. Two and a half-dimensional forward gravity models, based on the Talwani method, are used to calculate predicted gravity based on geometries and densities of subsurface bodies (our code was written by D. Roberts, and is a rewrite of tal.25dgrav by S.F. Lai; Talwani et al., 1959; Cady, 1980). We note that 2.5D models cannot illustrate the complexity of a three-dimensional system and therefore interpreting geologic features based on our models can be difficult. We limit our geologic interpretations to features that trend orthogonally to our profiles or have previously been studied. Geometries and densities of subsurface bodies modeled in previous studies are used as starting models in this study. The starting model for the San Luis basin (Fig. 2) comes from Lindsey et al. (1983), Trevino et al. (2004), and Grauch & Keller (2004). The starting model for the Albuquerque basin comes from Russell and Snelson (1994) and Keller and Baldridge (1999) (Fig. 3b). The starting model for the Tularosa basin (Fig. 4) comes from Healey et al. (1976), Russell and Snelson (1994), and Koning (1999). The ranges of densities in our models come from the starting models: 2.3-2.4 g/cm^3 for Mesozoic and Cenozoic sediment, 2.4-2.55 g/cm^3 for Paleozoic sediment, and 2.7-2.8 g/cm^3 for Precambrian basement. We note that the models are sensitive to the density structure and cannot inherently distinguish rock packages of varying age. In addition, Paleozoic stratigraphy derived from Grant and Foster (1985) was incorporated into the models to increase accuracy. Input parameters for the Talwani code include (a) geometries of subsurface bodies defined by x,y coordinates, (b) densities of these bodies with respect to a 2.7 g/cm^3 background density, and (c) distances to which bodies are projected in and out of the plane of the profile. Subsurface bodies at the edges of our profiles were extended laterally up to 800 km on each side of the basin in order to minimize edge effects.

GRAVITY MODEL RESULTS

San Luis Basin

The San Luis basin is the northern-most basin considered in this study (Fig 1). The San Juan and Tusas Mountains form the western edge of the basin and the high-standing Sangre de Cristo Mountains flank the eastern edge. The Sangre de Cristo Mountains are a series of thrust-faulted folds that originated during the Laramide orogeny (Lindsey et al., 1983; Lindsey, 1997). Located at the base of these mountains is the master normal fault of the basin, the Sangre de Cristo fault, which is interpreted to be a reactivated Laramide fault (Lindsey et al., 1983). The San Luis basin is about 10-12 km wide at its northernmost extent, but widens to about 75 km near Alamosa, Colorado (Keller et al., 1984). Just north of Alamosa the basin is split into two sub-basins separated by the intra-basin Alamosa horst (Brister and Gries, 1994; Grauch and Keller, 2004) which separates the Monte Vista and Baca grabens. Aeromagnetic studies (Grauch and Keller, 2004) as well as recent gravity studies (Trevino et al., 2004) show a series of basin structures becoming more complex southward within the San Luis basin. Profile A, oriented E-W across the San Luis basin, shows two sub-basins, approximately 3-4 km deep, separated by the Alamosa horst. The western sub-basin fill is primarily sediments shed westward off a Laramide uplift whereas the eastern sub-basin fill is likely rift-related (Brister and Gries, 1994). The gravity signature associated with the Sangre de Cristo Mountains is anomalously low for the basement rock observed on the surface. Lindsey et al. (1983) created cross sections just north of Profile A showing the Precambrian basement rock of the Sangre de Cristo Mountains thrust on a series of faulted folds of Paleozoic strata. When this thrust zone is incorporated into the model, the predicted gravity closely models the observed gravity (Figs. 2a and 2b). We note that this profile crosses the Culebra embayment, where the mountain front faulting is more diffuse (Wallace, 2004), making interpretations of this gravity model more complex. Profile B, oriented north-south shows a 5-6 km deep intra-basin in the northern San Luis basin and the northern

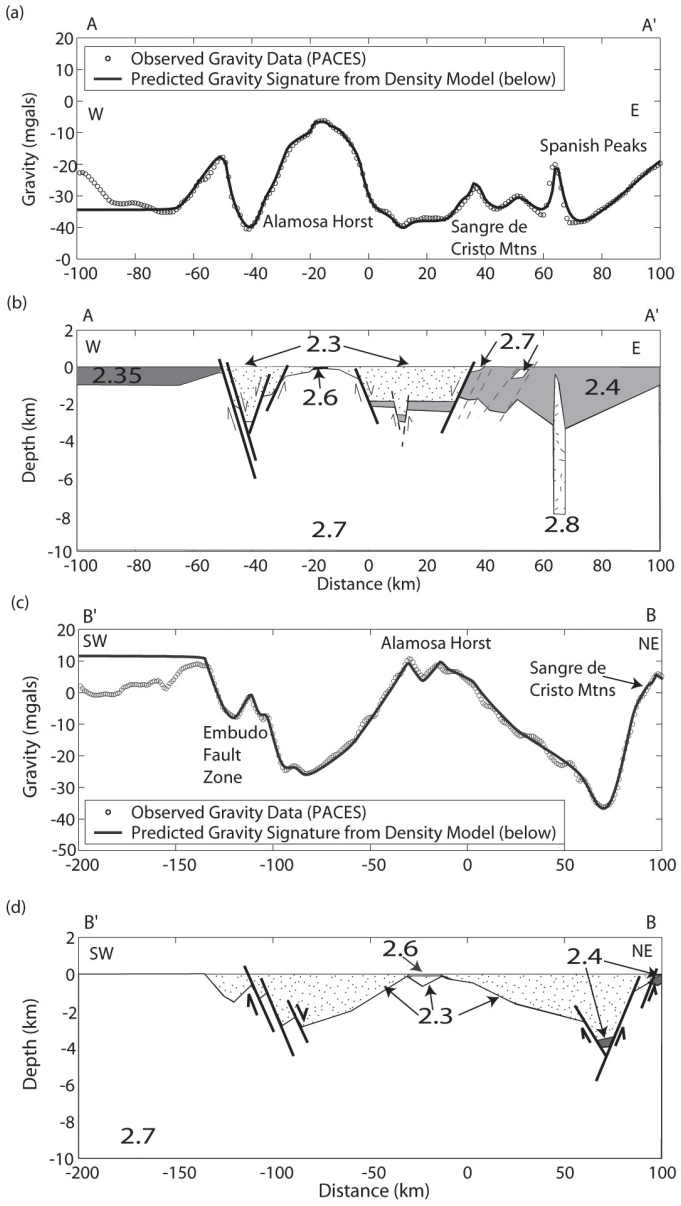

FIGURE 2. Observed and predicted gravity signatures across the San Luis basin. (a) Profile A and (b) Density model (in kg/m^3) on which predicted gravity signature is based. Two intra-basins are separated by the Alamosa horst. Note the low gravity anomaly associated with the Sangre de Cristo Mountains along the eastern edge of the basin. (c) Profile B and (d) density model on which the predicted gravity signature is based. Gravity anomaly associated with the Embudo Fault zone is apparent in the southern end of the profile.

part of the Alamosa horst to the south (Figs. 2c and 2d). The faults needed in these models are consistent with aeromagnetic and gravity maps of Grauch and Keller (2004) and with geological constraints discussed in Brister and Gries (1994).

Albuquerque Basin

The Albuquerque basin is a complex basin composed of three sub-basins. The two northern basins have an easterly tilt where as the southern sub-basin tilts to the west. The Albuquerque basin marks a transition between the narrow northern rift and the less-distinct southern rift, and connects the Española basin in the north with the Jornado del Muerto basin in the south (Fig. 1). The Albuquerque basin is one of the largest basins in the Rio Grande rift, faulted on nearly all sides (Connell, 2004). Subsidence within the basin is mostly controlled by normal north-south trending faults and the basin margins are defined by tilted flanking uplifts. The master fault zone of the Albuquerque basin is located on the eastern edge, along the Sandia, Manzanita, Manzano, Los Pinos Mountains, and along the western edge of the basin along the fronts of the Ladron Mountains and Lucero uplift. The faults making up this zone step down relatively shallow structural benches within the basin that separate deep intrabasinal areas (Grauch, et al., 1999). The northwestern edge of the Albuquerque basin is bounded by north-south trending faults that have significantly less offset than the eastern faults (Connell, 2004). The Albuquerque basin is the most-well studied of the three basins considered and, previous geophysical and geological studies model basin geometry (Russell and Snelson, 1994; Keller and Baldridge, 1999). In this paper we refine geometry along our study profile using more recent gravity data acquired in the basin that has been incorporated into the PACES gravity dataset. The gravity data for the Albuquerque basin show a gravity high at the center of the basin (Fig. 3a). Two hypotheses were examined in this study of the Albuquerque basin—an intrusion-driven anomaly, and a faulted basin floor allowing higher density basement rock closer to the surface. Gravity models are not unique and therefore cannot determine which hypothesis is correct. However, when coupled with the geologic models of Connell (2004) and Maldonado et al. (1999) as well as seismic studies of Russell and Snelson (1994) an intrusion large enough to create the observed anomaly appears unlikely. Therefore the basin structure model (Fig. 3c) was adopted for the remainder of this study. Based on the model, the depth of the basin is about 8 km, consistent with earlier work by Keller and Baldridge (1999) (Fig. 3b).

Tularosa Basin

The Tularosa basin is one in a series of laterally-adjacent basins in the wide, southern section of the Rio Grande rift where the rift begins to merge with the southern Basin and Range province (Fig. 1). In this region the rift has undergone about 50 percent extension distributed over multiple basins (Chapin and Cather, 1994). The Tularosa basin is located southeast of the Albuquerque basin between the Sacramento Mountains to the east and the San Andres Mountains to the west. Both mountain ranges are fronted by high-angle (~60 degree dipping) normal faults (Healey et al., 1978), the best-studied being the multi-segmented Alamagordo fault along the Sacramento Mountains (Koning, 1999). The Sierra Blanca Mountains and the Carrizozo Volcanic Field flank the northeastern edge of the basin. The northwestern edge is flanked by the Oscura Mountains. Most previous studies of the Tularosa basin concentrate on the southern and central basin. Previous gravity studies (Adams and Keller, 1994) depict the central section of the Tularosa basin as two graben-block struc-

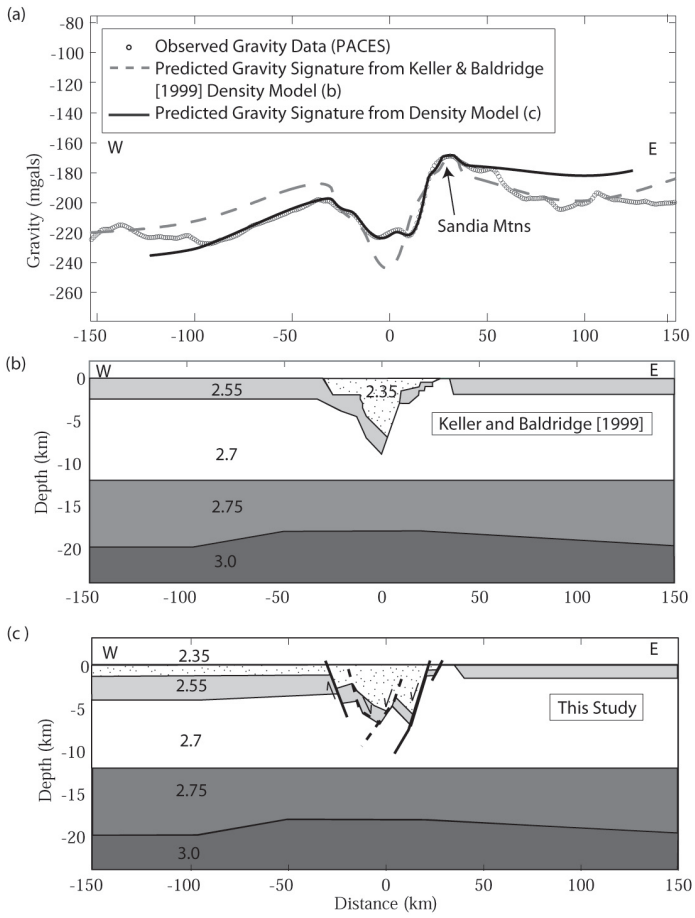

FIGURE 3. (a) Observed gravity signature across profile C (Albuquerque basin) as well as (b) the predicted density model from Keller and Baldridge (1999), and (c) density model of this study.

tures separated by a nearly symmetric horst. The White Sands Missile Range is located in the northern Tularosa basin, limiting access to data from this section of the basin. Therefore, in this study we examine three intersecting profiles that cross the Oscura Mountains into the northern basin to help examine overall structure of the basin. Profiles D and E are oriented northwest-southeast across the Oscura Mountains. Two steeply dipping (approximately 60°) normal faults that have not previously been mapped are required at the base of the Oscura mountain range in order to match observed gravity values (Figs. 4b and 4d). Profile D also shows several basin structures, modeled as normal faults, at the southern side of the basin (Figs. 4a and 4b). Profile E shows a more symmetric basin bounded by the Alamagordo fault along the Sacramento Mountains in the southeast (Figs. 4c and 4d) (Koning, 1999). Both profiles show that the basin is about 2-3 km deep. Profile F was modeled in order to better examine the basin structures revealed in Profile D (Figs. 4e and 4f). Profile F shows two sub-basins separated by an intra-basin horst. The presence of this horst is supported by studies of the Alamagordo fault by Koning (1999) as well as the presence of Paleozoic rocks on the surface less than one kilometer southeast of the profile line and is consistent with the previous gravity models of Adams and Keller (1994). Both sub-basins are approximately 2-3 km deep. There is a gravity high in the center of the western sub-basin, which has been modeled as a narrow intrusion. The anomaly is too narrow to be modeled as a basin structure. Also apparent in the western part of Profile F is anomalously high observed gravity associated with the San Andres Mountains along the western edge of the basin. This high density body may reflect the presence of an intrusion in this region, or simply a denser heterogeneous basement rock. As noted above, due to the inherent non-uniqueness of our gravity modeling, further work is required to interpret the large gravity contrast between the San Andres Mountains and the Tularosa basin.

FLEXURE-MODELING PROCEDURES

Extensional unloading along normal faults of continental rifts may result in a flexural response in the footwall, causing characteristically asymmetric rift flanks with steep faces towards the basin and gentle broad slopes on the other side (Vening-Meinesz, 1950; Wernicke and Axen, 1988). Previous studies have determined that flexurally induced rift-flank uplift may have played an important role in the creation of the high-relief flanks in the rift, including the Sandia Mountains (Roy et al., 1999) and the Sacramento Mountains (Brown and Philips, 1999). In this study we re-examined these mountain ranges in the context of flexural uplift and created flexure models of the Sangre de Cristo range in an attempt to understand the role of flexure within individual basins and how it changes throughout the length of the rift. Topography and gravity data were extracted by the same method used in the gravity models, however the gravity data used in the flexure models are not detrended to remove long-wavelength signals. The topography and gravity profiles represent average topography and gravity over a 10 km-wide swath in order to avoid any local anomalies in the data and obtain a more representative dataset for the rift flank.

Our models calculate the one-sided deflection of a semi-infinite, uniform rigidity plate, where the plate end is at the topographic crest of each mountain range considered (Fig. 5a). The modeling technique used is based on Kruse and Royden (1994) and Roy et al. (1996). This technique uses both gravity and topography data as constraints in a least-squares inversion for plate flexure. We assume that in the region of the footwall affected by flexural uplift, the initial elevation of the plate is unknown and we solve for the best-fit initial plate elevation. In the parts of the profiles that are several hundred kilometers from the plate-edge (taken to coincide with the topographic crest of the footwall flank), we solve for variable initial topography on the plate, assuming that present-day topography represents a combination of initial topography and flexural effects. For each basin, multiple models were made using different elastic plate thicknesses to determine the best-fit flexure model, assuming a Young's modulus E = 8.1 x 10^{10} Pa and Poisson's ratio ν = 0.25.

Flexure models were created along east-west trending profiles: at ~37.25°N across the San Luis basin; at ~35.05°N and ~34.75°N in the Albuquerque basin; and at ~33.20°N and ~32.63°N across the Tularosa basin (Fig. 1). The flexure methodology for each profile involves choosing a subset of the rift-flank topography

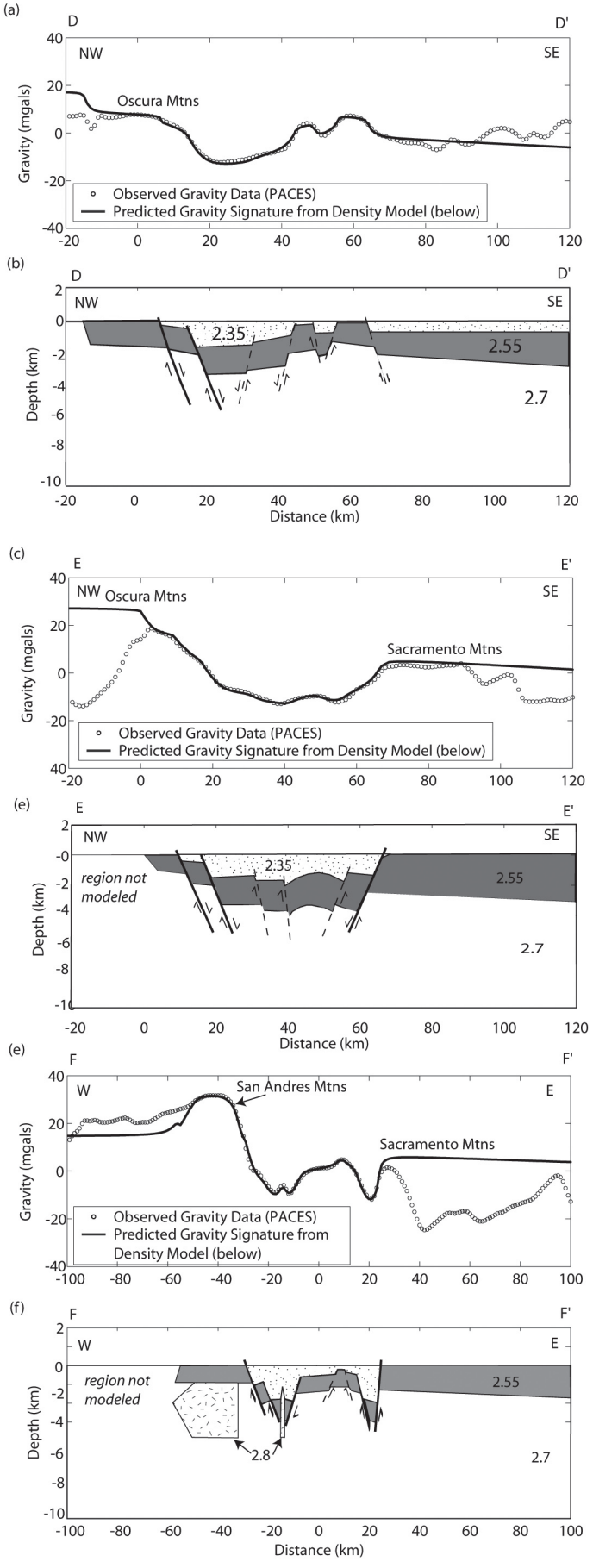

(immediately adjacent to the basin) to represent a proxy for plate deflection and invert for the flexure model that jointly fits (in a least-squares sense) both the deflection and the gravity data. An adjustable parameter in the model is the relative weighting between the deflection and the gravity data. In all cases, we find that reasonable flexural fits to topography in the footwall are obtained only when the gravity data are weighted much lower than the deflection data. For each basin, we experimented with varying the part of the topographic flank of the footwall used as a proxy for deflection and ran our calculations for a range of effective elastic plate thicknesses (rigidities) and chose the best-fitting rigidity.

As a check on the validity of the flexural model, the plate-end load required for our best-fitting footwall flexure is then compared to the loads estimated from basin geometry and upper crustal thinning (Fig 5). Following the method in Roy et al. (1996), we use the best-fit flexural rigidity from footwall flexure to calculate the response of a continuous plate deformed to match the footwall rift-flank. In the region of the basin and hanging wall, this deflection is an estimate of the isostatic response of an initially flat plate, with the same rigidity as the footwall, during extension (Fig. 5b). The assumption built-in to this procedure is that the rigidity of the plate was uniform across the future hanging wall and footwall blocks prior to extension, which is a reasonable first-order approximation. The area beneath this deflection curve and the present-day topography is an approximate measure of the "missing mass" or material removed by extension, and hence the end-load on the footwall plate (Fig. 5b and 5c; Roy et al., 1996; Roy et al., 1999). If the plate end-load estimated by the material removed calculation matches that inferred from the footwall rift-flank uplift model, then flexure is a viable interpretation for the high rift-flank elevations.

Following Roy et al. (1996), we assume that the material removed during extension can be inferred from the geometry of the plate response in the hanging wall (using the present-day basin geometry to take into account the material replaced during basin deposition). The material removed thus represents variable upper crustal thinning (Fig. 5c). Assuming Airy isostasy, we can use the upper crustal thinning to derive a *maximum* estimate of horizontal crustal extension (Fig. 5c), which can be directly compared to geologic estimates. If this flexure-based estimate of crustal extension is consistent with geologically derived estimates of extension, then we take this as added corroboration of the flexural interpretation of footwall rift-flank uplift.

FIGURE 4. (a) Observed and predicted gravity signatures across profile D (Tularosa basin). (b) Density model on which predicted gravity signature is based. Densities are given in kg/m^3. Two previously unmapped normal faults are modeled at the base of the Oscura Mountains. (c) Profile E and (d) density model on which predicted gravity signature is based. The model indicated an asymmetric basin with the Alamagordo Fault in the east along the Sacramento Mountains, and the two previously unmapped faults found in Profile D in the west along the Oscura Mountains. (e) Profile F and (f) density model on which predicted gravity signature is based. Two intra-basins are separated by an intra-basin horst (consistent with Adams and Keller (1994)). Note the high gravity anomaly associated with the San Andres Mountains in the west and the high gravity anomaly within the western-most sub-basin.

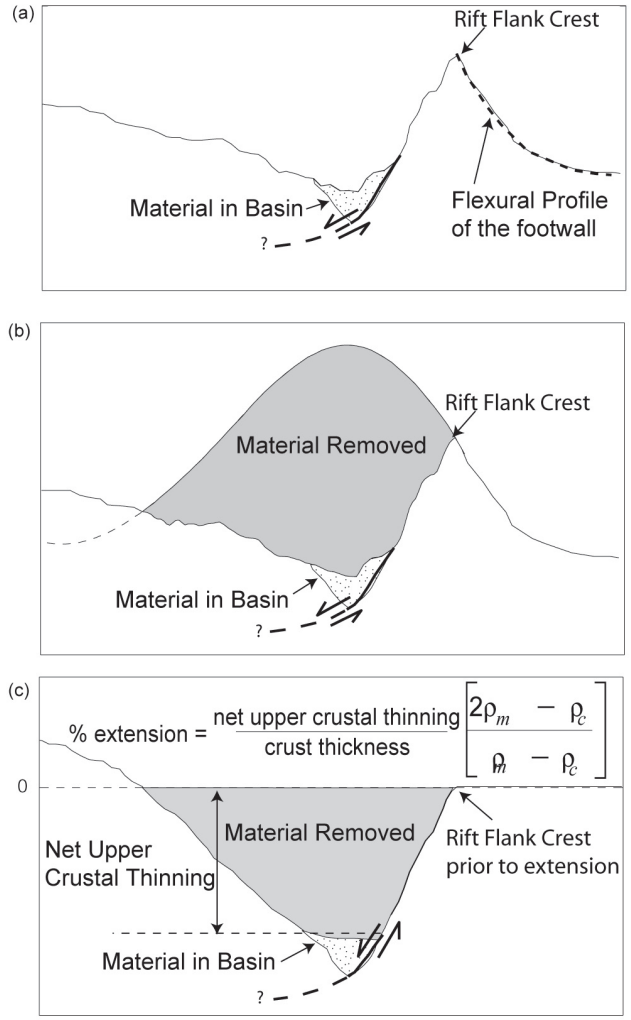

FIGURE 5. Flexure cartoons to illustrate the modeling technique: (a) Topographic data points are used as a proxy for deflection in the footwall to calculate the best-fit flexure profile; (b) Using the best-fit flexural rigidity from footwall flexure profile we calculate the response of a continuous plate deformed to match the footwall rift-flank. The area beneath this deflection curve and the present-day topography is an approximate measure of the "material removed" represented by effects of extension, and hence the end-load on the footwall plate; (c) The "material removed", excluding the isostatic response to unloading, represents the net upper crustal thinning which is then used to calculate the a maximum estimate of percent extension assuming Airy compensation.

FLEXURE MODEL RESULTS

The results of our flexure modeling show that in all cases, flexural fits to the topography of the footwall flank can be obtained; however, our comparisons to estimated loads show that flexure is not a viable process in all basins (Fig. 6). The best-fit plate thickness for both the northern and southern Albuquerque basin is T_e=5 km (rigidity D= 9 x 10^{20} Nm; Table 1). The estimated plate-end loads from footwall flexure and from inferred hanging wall isostatic responses agree with each other (Table 1) and with the earlier study by Roy et al. (1999), and the estimated crustal extension from flexure agrees with geologic estimates (Table 1).

Discussing the basins from north to south in the rift, we find that although a reasonable flexural fit to the rift-flank topography of the San Luis basin is found for T_e=5 km (rigidity D= 9 x 10^{20} Nm; Fig. 6), the flexure model is not a valid one. This is because the low plate rigidity predicts concentrated isostatic responses within the basin and in the hanging wall block. Therefore, the estimated plate end-load from the material removed is smaller than the end-load required to drive flexure by several orders of magnitude (Table 1). Additionally, the estimated horizontal extension (based on our constraints on basin geometry) is 38% across the southern San Luis basin, which is much greater than the geologic estimate of 8-12%.

In the Albuquerque and Tularosa basins, we conclude that flexure is a valid process for generating the elevated rift-flank topography (Fig. 6). Our results for the northern and southern Albuquerque basin suggest a best-fit effective elastic plate thickness of T_e=5 km (D= 9 x 10^{20} Nm) along both profiles across the basin (Fig. 6), consistent with Roy et al. (1999). The best-fit effective elastic plate thickness in the Tularosa basin is higher than that in the Albuquerque basin T_e=20 km (D = 6 x 10^{27} Nm; Fig.6). In both the Albuquerque and Tularosa basins, the estimated plate end-loads from the material removed inferred from hanging wall responses is on the same order of magnitude as the end-load required for footwall flexure (Table 1). We note that the plate-end load inferred from the material removed for the Tularosa basin profiles represents end-loads distributed over a broad region, encompassing the Jornada del Muerto and the Tularosa basin (Fig. 1; Table 1). As this load is distributed over two basins, we suspect that the actual load supported by the plate in the footwall of the Tularosa basin is lower, more consistent with the loads required to drive footwall flexure (Table 1).

The flexure-based estimate for crustal extension is 14% in the northern Albuquerque basin (geologic estimate of 17%) and is at least 30% in the southern Albuquerque basin (geologic estimate of at least 28%), and 28-34% in the Tularosa basin (geologic estimate of ~ 40-50% extension distributed across multiple basins; Table 1). These results are consistent with previous models in the Albuquerque (Roy et al., 1999) and Tularosa basins (Brown and Phillips, 1999), but take the investigation one step farther by evaluating the along-strike variability and applicability of flexure as a means of generating high rift-flank topography in the Rio Grande rift as a whole.

CONCLUSIONS

Our results suggest that, although rift-flank topography surrounding the Rio Grande rift may be modeled by fitting a flexural curve representing plate deflection, the plate-end loads and the implied net crustal extension must be considered to thoroughly evaluate the plausibility of flexure during extension. We note that in using topography as a proxy footwall deflection, we are making a major assumption that erosional processes do not significantly affect the topographic profiles over 20-50 km scales. We have investigated models where the deflection profile consists of points only on the upper and lower enveloping surfaces

TABLE 1. Summary of results for flexure models of each profile, including the effective elastic plate thickness (T_e) used in each profile, end load estimates from the footwall and material removed calculations, the extension estimates from this study and from geologic constraints (Chapin and Cather, 1994).

Basin	Latitude	Best-fit Te(km) using D= 9x1020 Nm	End-load required by footwall flexure (N/m)	End-load inferred from material removed (N/m)	% extension calculated from material removed	% extension estimated from geology (Chapin and Cather, 1994)	Flexure Plausible?
San Luis	37.25ºN	5	1.4325 x 10^13	8.9581 x 10^11	~38 %	8 - 12 %	no
Albuquerque	35.05ºN	5	1.1250 x 10^11	3.5471 x 10^11	~14 %	17 - 28 %	yes
Albuquerque	34.75ºN	5	3.7500 x 10^11	8.7897 x 10^11	~30 %	17 - 28 %	yes
Tularosa	33.20ºN	20	2.2500 x 10^11	1.2381 x 10^12	~34 %	40 - 50 % *	yes
Tularosa	32.63ºN	20	3.00 x 10^11	1.5698 x 10^12	~28 %	40 - 50 % *	yes

* Note: These estimates reflect the percent extension distributed over a broad region encompassing multiple basins. Our estimates of extension reflect the extension associated with the Tularosa basin.

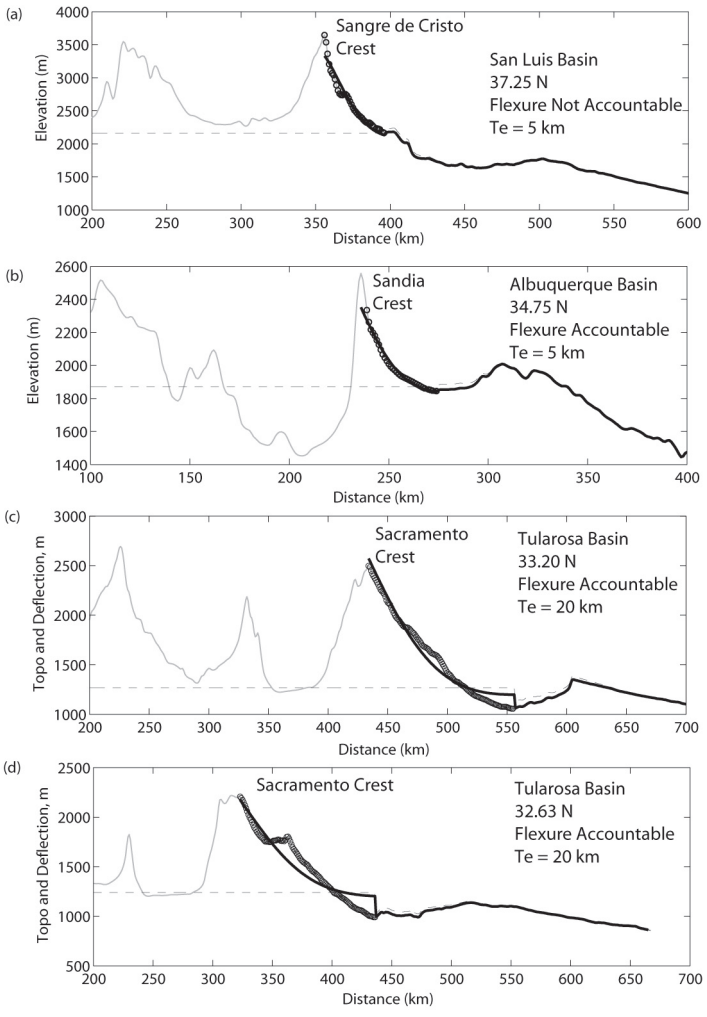

FIGURE 6. Best-fit footwall flexure curves (solid black line) with D = 9 x 10^{20} Nm for (a) San Luis basin, 37.25º N, with T_e = 5 km; (b) Albuquerque basin, 35.05º N, with T_e = 5 km, and (c) 34.74º N, with T_e = 5 km; and (d) Tularosa basin, 33.20º N, and (e) 32.63º N with T_e = 20 km. Topography shown by solid grey line, the circles represent the deflection data points used to calculate the flexure curve. Calculated average elevation prior to footwall flexure is shown in the dashed line.

of the footwall flank, and our results remain unchanged. We find that flexural responses to crustal extension may have generated elevated rift-flanks in the central and southern parts of the Rio Grande rift, within and south of the Albuquerque basin. In the northern, narrow portion of the Rio Grande rift, we suggest that much of the present-day high elevations surrounding the rift basins may be unrelated to isostatic responses to crustal extension. One possible origin for high rift-flank elevations in the northern Rio Grande rift is pre-rift, Laramide topography. We note that this conclusion is consistent with major Laramide structures in central Colorado (Hamilton, 1988) as well as with recent compilations of apatite fission-track data that show Laramide-age rock cooling in the Sangre de Cristo Mountains in the northern rift (Kelley and Chapin, 1995), and local cooling during rift extension in the Sandia Mountains (House et al., 2003) and Ladron Mountains (Kelley and Chapin, 1995; and compilation in Roy et al., 2004).

We conclude that flexural response to extension is a dominant tectonic process over a short wavelength surrounding the Rio Grande rift, with effective elastic plate thickness a minimum of T_e=5 km (D= 9 x 10^{20} Nm) in the Albuquerque basin and T_e=20 km (D= 5.8 x 10^{22} Nm) in the Tularosa basin region and flexural wavelengths of α=29 to 81 km, respectively. Our results for the southern part of the rift are consistent with those of Brown and Phillips (1999), who found an average best-fit effective elastic plate thickness of 23 km in the footwall of the Tularosa basin. This result suggests that lithospheric strength in the southern, wider part of the rift (with basin depths of only 2-3 km in the Jornado del Muerto and Tularosa basins) may be greater than that in the narrow section encompassing the Albuquerque basin (>10 km deep in some places). This variation in plate rigidity is likely an important factor in controlling the mode of extension, although we note that there is a complex relationship between plate rigidity and width of the zone of continental extension (e.g., Buck, 1991; Buck et al., 1999). The low rigidity in the Albuquerque basin region and the anomalous depth of the basin may indicate a complex process of lithospheric weakening during extension, e.g., by necking and significant upper crustal faulting, influence of magmatic intrusions, etc. (Buck et al., 1999). Other important factors that control the mode of continental extension include the possibility of high heatflow and lower crustal flow which, in combination, can lead to a wide-rift mode of continental exten-

sion (Buck et al., 1999), and which may be more dominant in the southern Rio Grande rift/Basin and Range transition.

ACKNOWLEDGEMENTS

The authors are grateful to V.J.S. Grauch, G. Meyer, and J. Selverstone for comments and suggestions, and to S. Baldridge, S. Connell, and J. Geissman for thorough reviews. We also thank G.R. Keller and the PACES data center for access to the gravity data. This work was partially supported by NSF (EAR award #0408513 to MR).

REFERENCES

Adams, D. C., and Keller, G. R., 1994, Crustal structure and basin geometry in south-central New Mexico; *in* Keller, G. R. and Cather, S. M., eds., Basins of the Rio Grande rift: Structure, Stratigraphy, and Tectonic Setting: Geological Society of America, Special Paper 291, p. 5-25.

Balch, R., Hartse, H., Sanford, A., and Lin, K., 1997, A geographical extent of the Socorro midcrustal magma body: Seismological Society of America, Bulletin, v. 87, p. 174-182.

Brown, C. D. and Phillips, R. J., 1999, Flexural rift flank uplift at the Rio Grande rift, New Mexico: Tectonics, v. 18, no. 6, p. 1275-1291.

Brister, B.S., and Gries, R.R., 1994, Tertiary stratigraphy and tectonic development of the Alamosa basin (northern San Luis basin), Rio Grande rift, south-central Colorado; *in* Keller, G.R., and Cather, S.M., eds., Basins of the Rio Grande rift: Structure, stratigraphy, and tectonic setting: Geological Society of America, Special paper 291, p. 35-58.

Buck, W.R., 1991, Modes of continental lithospheric extension: Journal of Geophysical Research-Solid Earth, v. 96, no. B12, p. 20161-20178.

Buck, W.R., Lavier, L.L., and Poliakov, A.N.B., 1999, How to make a rift wide: Philosophical transactions of the royal society of London series A – Mathematical physical and engineering sciences, v. 357, no., 1753, p/ 671-690.

Cady, J. W., 1980, Calculation of gravity and magnetic anomalies of finite-length right polygonal prisms: Geophysics, v. 45, no. 10, p. 1507-1512

Chapin, C. E. and Cather, S. M., 1994,Tectonic setting of the axial basins of the northern and central Rio Grande rift; *in* Keller, G. R. and Cather, S. M., eds., Basins of the Rio Grande rift: Structure, Stratigraphy, and Tectonic Setting: Geological Society of America, Special Paper 291, p. 5-25.

Connell, S. D., 2004, Geology of the Albuquerque Basin and tectonic development of the Rio Grande Rift in north-central New Mexico; *in* Mack, G. H., and Giles, K.A., eds., The Geology of New Mexico: A geologic history: New Mexico Geological Society, Special Paper 11, p. 359-385.

Cordell, L., 1978, Regional geophysical setting of the Rio Grande rift: Geological Society of America Bulletin, v. 89, p. 1073-1090.

Dueker, K., Yuan, H., and Zurek, B., 2001, Thick-structured Proterozoic lithosphere of the Rocky Mountain region: GSA Today, v. 11, no. 12, p. 4-9.

Gao, W., Grand, S. P., Baldridge, W.S., Wilson, D., West, M., Ni, J. F., and Aster, R., 2004, Upper mantle convection beneath the central Rio Grande rift imaged by P and S wave tomography: Journal of Geophysical Research, v. 109, B03305, doi:10.1029/2003JB002743.

Grant, P.R., and Foster, R.W., 1985, Future petroleum provinces in New Mexico—discovering new reserves; *prepared for* the New Mexico Research and Development Institute: New Mexico Bureau of Mines and Mineral Resources, p. 12-23.

Grauch, V. J. S., Gillespie, C. L., and Keller, G. R., 1999, Discussion of new gravity maps for the Albuquerque basin area: New Mexico Geological Society, 50th Field Conference Guidebook, p. 119-124.

Grauch, V.J.S., and Keller, G.R., 2004, Gravity and Aeromagnetic expression of tectonic and volcanic elements of the southern San Luis basin, New Mexico and Colorado: New Mexico Geological Society, 55th Field Conference Guidebook, p. 230-243.

Gregory, K.M., and Chase, C.G., 1994, Tectonic and climatic significance of a late Eocene low-relief, high-level geomorphic surface, Colorado: Journal of Geophysical Research, v. 99, p. 20,141-20,160.

Hamilton, W.G., 1988, Laramide crustal shortening; *in* Schmidt, C.J., and Perry, W.J., eds. Interaction of the Rocky Mountain foreland and the Cordilleran thrust belt: Geological Society of America, p. 27-39.

Healey, D. L., Whal, R. R., and Currey, F. E., 1978, Gravity survey of the Tularosa valley and adjacent areas, New Mexico: United States Department of the Interior, Geological Survey, Open-file report 78-309.

House, M. A., Kelley, S., and Roy, M., 2003, Refining the footwall cooling history of a rift flank uplift, Rio Grande rift, New Mexico: Tectonics, v. 22, no. 1060, doi: 10.1029/2002TC00148.

Humphreys, E., Hessler, E., Dueker, K., Farmer, C., Ersley, E., and Atwater, T., 2003, How Laramide age hydration of North American lithosphere by the Farallon slab controlled subsequent activity in the western United States: International Geology Review, v. 45, p. 575-595.

Keller, G. R., Cordell, L., Davis, G. H., Peeples, W. J., and White, G., 1984, A geophysical study of the San Luis basin, New Mexico: Geological Society, 35th Field Conference Guidebook, p. 51-57.

Keller, G. R., Morgan, P., and Seager, W. R., 1990, Crustal structure, gravity-anomalies and heat-flow in the southern Rio-Grande rift and their relation to extensional tectonics: Tectonophysics, v. 14, no. 1-2, p. 21-37.

Keller, G. R., and Baldridge, W. S., 1999, The Rio Grande rift: A geophysical overview: Rocky Mountain Geology, v., 34, no. 1, p. 121-130.

Kelley, S. A., and Chapin, C. E., 1995, Apatite fission-track thermochronology of southern Rocky Mountain—Rio Grande rift-western High Plains provinces: New Mexico Geological Society, 46th Field Conference Guidebook, p. 87-96.

Koning, D.J., 1999, Fault segmentation and paleoseismicity of the southern Alamogordo fault, southern Rio Grande rift, New Mexico: Thesis (M.S.)-University of New Mexico, Dept. of Earth and Planetary Sciences, p. 20-79.

Kruse, S., and Royden, L.H., 1994, Bending and unbending of an elastic lithosphere: the Cenozoic history of the Apennine and Dinaride foredeep basins: Tectonics, v. 13, p. 278-301.

Lindsey, D. A., Johnson, B. R., and Andriessen, P. A. M., 1983, Laramide and Neogene structure of the northern Sangre de Cristo range, south-central Colorado: Rocky Mountain Association of Geologists, p. 219-228.

Lindsey, D. A., 1997, Laramide structure of the Central Sangre de Cristo Mountains and adjacent Ration Basin, southern Colorado: The Mountain Geologist, v. 35, no. 2, p. 55-70.

Maldonado, F., Connell, S.D., Love, D.W., Grauch., V.J.S., Slate, J.L., McIntosh, W.C., Jackson, P.B., and Byers, F.M., Jr., 1999, Neogene geology of the Isleta Reservation and vicinity, Albuquerque basin, central New Mexico: New Mexico Geological Society, 50th Field Conference Guidebook, p. 175-188.

Roy, M., Royden, L. H., Burchfiel, B. C., Tzankovt, T., and Nakovt, R., 1996, Flexural uplift of the Stara Planina range, central Bulgaria: Basin Research, v. 8, p. 143-156.

Roy, M., Karlstrom, K., Kelley, S., Pazzaglia, F., and Cather, S. M., 1999, Topographic setting of the Rio Grande rift, New Mexico: assessing the role of flexural "rift-flank uplift" in the Sandia Mountains: New Mexico Geological Society, 50th Field Conference Guidebook, p. 167-174.

Roy, M., Kelley, S., Pazzaglia, F., Cather, S. M., House, M., 2004, Middle Tertiary buoyancy modification and its relationship to rock exhumation, cooling, and subsequent extension at the eastern margin of the Colorado Plateau: Geological Society of America, Geology, v. 32, no. 10, p. 925-928.

Russell, L., R., and Snelson, S., 1994, Structure and tectonics of the Albuquerque Basin segment of the Rio Grande rift: Insights from reflection seismic data; *in* Keller, G., R., and Cather, S. M., eds., Basins of he Rio Grande Rift: Structure, Stratigraphy, and Tectonic Setting: Geological Society of America, Special Paper 291, p. 83-112.

Sanford, A.R., Balch, R., and Lin, K., 1995, A Seismic anomaly in the Rio Grande rift near Socorro, New Mexico (abs.): Seismological Research Letters, v. 66, no. 2, p.44.

Talwani, M., Worzel, J. L., and Landisman, M.G., 1959, Rapid gravity computations for two-dimensional bodies with application to the Mendocino submarine fracture zone (Pacific Ocean), J. Geophys. Res., v. 64, no. 1, p. 49-59.

Trevino, L., Keller, G.R., Andronicos, C., and Quezada, O., 2004, Rootless mountains and gravity lows in the Sangre de Cristo Mountains, southern Colorado-northern New Mexico: New Mexico Geological Society, 55th Field Conference Guidebook,, p. 264-271.

Vening-Meinesz, F.A., 1950, Les 'grabens" africains, resultat de compression ou de tension dans la croute terrestre?: Bulletin of the Royal Colonial Institute of Belgium, v. 21, p. 539-552.

Wallace, A.R., 2004, Evolution of the southeastern San Luis basin margin and the Culebra embayment, Rio Grande rift, southern Colorado: New Mexico Geological Society, 55th Field Conference Guidebook,p. 181-192.

Wernicke, B., and Axen, G.J., 1988, On the role of isostasy in the evolution of normal fault systems: Geology, v. 16, p. 848-851.

Wessel, P., and Smith, W.H.F., 1991, Free software helps map and display data: AGU EOS Trans., v. 72, p. 441.

West, M., Ni, J., Baldridge, W. S., Wilson, D., Aster, R., Gao, W., and Grand, S., 2004, Crust and upper mantle shear wave structure of the southwest United States: Implications for rifting and support for high elevation: Journal of Geophysical Research, v., 109, B03309, doi:10.1029/2003JB002575.

Wilson, D., Aster, R., West, M., Ni, J., Grand, S., Gao, W., Baldridge, W.S., Semken, S., and Patel, P., 2005, Lithospheric structure of the Rio Grande rift: Nature, v. 433, no. 7028, doi:10.1038/nature03297.